Atmos. Chem. Phys. Discuss., https://doi.org/10.5194/acp-2018-1042
Manuscript under review for journal Atmos. Chem. Phys.
Discussion started: 15 November 2018
© Author(s) 2018. CC BY 4.0 License.

Atmospheric Chemistry and Physics Discussions

Atmospheric radiocarbon measurements to quantify CO_2 emissions in the UK from 2014 to 2015

Angelina Wenger[1,4*], Katherine Pugsley[1], Simon O'Doherty[1*], Matt Rigby[1], Alistair J. Manning[1,2], Mark Lunt[3], Emily White[1]

[1]School of Chemistry, University of Bristol, Bristol, BS8 1TS, UK
[2]Met Office, Exeter, Devon, EX1 3PB, UK
[3]School of GeoSciences, University of Edinburgh, UK
[4] Department of Environmental Science and Analytical Chemistry (ACES), Stockholm University, Stockholm, Sweden
Correspondence to: Angelina Wenger (aw12579@my.bristol.ac.uk), Simon O'Doherty (s.odoherty@bristol.ac.uk)

Abstract

We present $^{14}CO_2$ observations and related greenhouse gas measurements at a background site in Ireland and a tall-tower site in the east of the UK that is more strongly influenced by fossil fuel sources. These data have been used to calculate the contribution of fossil fuel sources to atmospheric CO_2 mole fractions from the UK and Ireland. Corrections were calculated and applied for $^{14}CO_2$ emissions from the nuclear industry and other sources such as biospheric emissions that are in disequilibrium with the atmosphere. Measurements at both sites were found to only be marginally affected by $^{14}CO_2$ emissions from nuclear sites. Over the study period of 2014 – 2015, the biospheric correction and the correction for nuclear $^{14}CO_2$ emissions were similar, at 0.4 and 0.3 ppm fossil-fuel CO_2 ($ffCO_2$)-equivalent, respectively. The observed $ffCO_2$ at the site was not significantly different from simulated values based on the EDGAR 2010 bottom-up inventory. We explored the use of high-frequency CO observations as a tracer of $ffCO_2$ by deriving a constant $CO_{enhanced}/ffCO_2$ ratio for the mix of UK fossil fuel sources. This ratio was found to be 5.7 ppb ppm^{-1}, close to the value predicted using inventories and the atmospheric model of 5.1 ppb ppm^{-1}. The site in the east of the UK was strategically chosen to be some distance from pollution sources so as to allow for the observation of well-integrated air masses. However this, and the large measurement uncertainty in $^{14}CO_2$, lead to a large overall uncertainty in the $ffCO_2$, being around 1.8 ppm compared to typical enhancements of 2 ppm.

1 Introduction

The level of carbon dioxide (CO_2) in the atmosphere is rising because of anthropogenic emissions, leading to a change in climate (IPCC, 2014; Le Quéré et al., 2018). Robust quantification of anthropogenic fossil fuel CO_2 ($ffCO_2$) emissions is vital for understanding the global and regional carbon budgets. However, biospheric fluxes are typically an order of magnitude larger than anthropogenic emissions (Le Quéré et al., 2018), which makes it difficult to utilise CO_2 observations in a "top-down" approach to estimate $ffCO_2$ emissions (Nisbet and Weiss, 2010). For this reason, most $ffCO_2$ emission estimates use bottom-up methods, based on inventories and process models (Gurney et al., 2017; van Vuuren et al., 2009; Zhao et al., 2012). These methods take into consideration factors such as the reported energy usage, the carbon content of the fuel and oxidation ratios (BEIS, 2018; Friedlingstein et al., 2010; Le Quéré et al., 2016). While these CO_2 emission inventories are considered to

© Author(s) 2018. CC BY 4.0 License.

be reasonably accurate, the quality of them is dependent on the statistics and reporting methods. In high income countries, uncertainties are estimated to be around 5 %, whereas, in low-middle income countries, these uncertainties can exceed 10 % (Ballantyne et al., 2015). However, distributing these emissions in space and time adds additional uncertainty, potentially leading to uncertainties on the order of 50 % (Ciais et al., 2010). According to bottom-up estimates in the UK in 2016, CO_2 emissions accounted for 81 % of all of the UK's greenhouse gas emissions (BEIS, 2018).

Unstable isotope measurements can provide a way of disentangle different sources, and directly quantify $ffCO_2$. Radiocarbon (^{14}C, half-life 5700±30 years (Roberts and Southon, 2007)) is produced in the stratosphere and subsequently oxidised to CO_2 (Currie, 2004). It is integrated into other carbon pools that have a relatively fast carbon exchange with the atmosphere, such as the biosphere and the surface ocean. Fossil fuels, having been isolated from the atmosphere for millions of years, are completely depleted in ^{14}C. Burning fossil fuels, therefore, causes a depletion in $^{14}CO_2$ that can be observed in the atmosphere, a phenomenon known as the Suess effect (Suess, 1955). Previously, $^{14}CO_2$ has been used to estimate fossil fuel emissions in the USA, Canada, New Zealand and some European countries (Bozhinova et al., 2016; Graven et al., 2012; Levin et al., 2003; Miller et al., 2012; Turnbull et al., 2009; Vogel et al., 2013; Xueref-Remy et al., 2018). However, it has not yet been used in the UK, partly because it was thought that the relatively high density of nuclear power plants emitting pure $^{14}CO_2$ would mask the depletion from fossil fuel burning. Previous studies suggest that this masking effect is particularly strong in the UK as the most prevalent type of nuclear power plant, Advanced Gas Reactors (AGR), have comparatively high $^{14}CO_2$ emissions (Bozhinova et al., 2016; Graven and Gruber, 2011). In previous studies, parametrized ^{14}C emissions were used, calculated by relating the power production of a nuclear power plant with a plant-type-specific emission factor. However, Vogel et al., 2013 showed that 14-day integrated atmospheric $^{14}CO_2$ observations in a region of Canada with high nuclear $^{14}CO_2$ emissions, could be better simulated using the reported monthly emissions from nuclear power plants, instead of the parameterized values. Reported emissions are likely better than parameterized values, as $^{14}CO_2$ emission from nuclear power plants can vary depending on operational parameters as well as the presence of fuel or cooling agent impurities.

Although $^{14}CO_2$ is an important tracer for fossil fuel CO_2 emissions, measurements are sparse. This is primarily because of the cost and time required per sample. This has motivated researchers to combine $^{14}CO_2$ observations with other tracers, such as carbon monoxide (CO) to improve temporal coverage (Gamnitzer et al., 2006; Levin and Karstens, 2007; Lopez et al., 2013; Miller et al., 2012; Turnbull et al., 2006, 2011). For example, high-frequency CO data has been used with $^{14}CO_2$ measurements to regularly calibrate the CO_{enh} (enhancement of CO from background concentration) to $ffCO_2$ ratio, based on weekly ^{14}C measurements in Europe (Berhanu et al., 2017; Levin and Karstens, 2007). However, using a CO_{enh}: $ffCO_2$ ratio to estimate higher frequency $ffCO_2$ can be challenging to implement even when using a well-calibrated ratio because the ratios of different sources and sinks impacting each measurement can vary considerably, as each source emits with a different CO : $ffCO_2$ ratio.

As part of the Greenhouse gAs Uk and Global Emissions (GAUGE) network (Palmer et al., 2018), weekly $^{14}CO_2$ measurements have been made at two sites between July 2014 and November 2015: Tacolneston, Norfolk (TAC) (52.51 °N, 1.13 °E), a site that is influenced by anthropogenic sources in England and Mace Head, Ireland (MHD) (53.32 °N, -9.90 °E), a background

© Author(s) 2018. CC BY 4.0 License.

site. From these observations, a time series of $ffCO_2$ is calculated, which is compared with simulated mole fractions. The influence of $^{14}CO_2$ from nuclear power plants and a correction required for the biospheric disequilibrium are also discussed. The CO_{enh}: $ffCO_2$ ratios at TAC are defined and their potential for calculating $ffCO_2$ is also evaluated.

2 Measurements

2.1 Site setup

The TAC tall tower measurement site was set up in 2012 as part of the UK DECC (Deriving Emissions linked to Climate Change) network. It is operated by Bristol University and the University of East Anglia. More details on the site and the network have been previously published (Stanley et al., 2018). The site is located in Norfolk, approximately 140 km north east of London. It was thought to be the most appropriate site in the UK DECC tall tower network for characterising $ffCO_2$ emissions from the UK using $^{14}CO_2$ because it has the most influence from fossil fuel sources and the least influence from nuclear power stations. The TAC tower site has 3 inlet heights; 54 m, 100 m and 185 m. CO is observed from the 100 m inlet once every 20 minutes, while all heights are sampled from for the CO_2 observations with a sampling frequency of ~3 seconds at an interval of 20 minutes per height. The highest height (185 m) was used for the $^{14}CO_2$ measurements as it was assumed that it would be the most representative for well-integrated air masses.

A background site is necessary for the $^{14}CO_2$ method, to evaluate the relative depletion caused by recently added emissions of $ffCO_2$. Different types of sites have been utilised as background in previous studies: unpolluted sites upwind of significant fossil CO_2 sources (Lopez et al., 2013; Miller et al., 2012), high altitude observations (Bozhinova et al., 2014; Levin and Kromer, 1997), free troposphere observations from an aircraft (Turnbull et al., 2011) and a mildly polluted site upwind of the polluted site (Turnbull et al., 2014). MHD, located on the west coast of Ireland, was used as the background site for this study and weekly sampling was performed when air masses were representative of clean air coming from the Atlantic. This study utilised both flask and, for some species, high-frequency in situ data from two sites (MHD and TAC), Table 1 gives an overview of the measurement techniques used, the calibration scales and the operator of the specific instrument or method. For CO, the flask and the in-situ data were reported on different calibration scales. Comparisons of co-located observations show that there is a significant difference between the two scales (supplementary material S1). Conversion between the CSIRO-98 and the WMO-2014 CO scale is non trivial as there is a time and concentration dependent difference between the two scales and no published conversion method is yet available. It was decided that only the in-situ data would be utilised for the CO ratio analysis, to avoid any effect these calibration scale differences might have on the CO ratio analysis. The measurements are reported as dry air mole fractions in ppm (µmol mol^{-1}) and ppb (nmol mol^{-1}).

Atmos. Chem. Phys. Discuss., https://doi.org/10.5194/acp-2018-1042
Manuscript under review for journal Atmos. Chem. Phys.
Discussion started: 15 November 2018
© Author(s) 2018. CC BY 4.0 License.

2.2 Sampling

The sampling procedure was based on the method used by the National Oceanic and Atmospheric Administration Carbon Cycle Greenhouse Gases (NOAA CCGG) (Lehman et al., 2013). At MHD, the sampling of an additional flask for $^{14}CO_2$ analysis was added to the existing weekly NOAA CCGG flask sampling collection. A manual instantaneous sampling module was constructed for TAC, using a KNF Pump to pressurise and a Stirling cooler (Shinyei MA-SCUCO8) set to 0°C to dry the sample. Additionally, a 7-micron particle filter was added to avoid contamination of the sampling module and a check valve in addition to a toggle valve to ensure that existing measurements at the site were not influenced. A selection of tests, including a side-by-side comparison with the NOAA CCGG sampling unit at MHD, were performed before deployment to TAC. At TAC, samples were collected weekly into 2 L glass flasks (NORMAG, Germany, based on the NOAA CCGG design).

3 Methods

3.1 NAME simulations

Mole fractions were simulated at each measurement site using the Lagrangian particle dispersion model NAME (Numerical Atmospheric dispersion Modelling Environment) developed by the UK Met Office (Jones et al., 2007). Hypothetical particles are released into the model atmosphere at a rate of 10,000 per hour at the location of the observation site and transported backward in time for 30 days. It is assumed that when a particle resides in the lowest 0 - 40 m of the model atmosphere, pollution from ground-based emission sources is added to the air parcel. The particle residence times in this surface layer are integrated over the 30-day simulation to calculate a "footprint" of each measurement that quantifies the sensitivity of the observation to a grid surrounding the measurement site (Manning et al., 2011). These footprints can be multiplied by flux fields to simulate the mole fraction due to each source at each instant in time. We separate CO_2 mole fractions at time t ($CO_{2,t}$) into a background concentration ($CO_{2\,bg,t}$) and a contribution from each source i:

$$CO_{2,t} = CO_{2\,bg,t} + \sum_i CO_{2,i,t} \quad (1)$$

The background concentration can be determined by applying statistical methods to high-frequency observations (Barlow et al., 2015; Ruckstuhl et al., 2012) or estimated by models (Balzani Lööv et al., 2008; Lunt et al., 2016). In this work, high-frequency data existed only for $^{12}CO_2$ but not its isotopes and there was no model-derived background available for the isotopes, therefore, MHD data was used as background for the simulation of all CO_2 isotopes. While $^{13}CO_2$ and $^{14}CO_2$ measurements in MHD were selectively sampled during clean air conditions (high wind speeds from the Atlantic Ocean) the high-frequency $^{12}CO_2$ data also contained pollution events. To exclude the pollution events, a rolling 15 percentile value (± 20 days) was calculated and used as $^{12}CO_2$ background. Similarly, for the $^{13}CO_2$ and $^{14}CO_2$ background rolling median values (± 30 days) were calculated. These rolling median values created a smoother seasonal cycle compared to using the closest observed value.

Atmos. Chem. Phys. Discuss., https://doi.org/10.5194/acp-2018-1042
Manuscript under review for journal Atmos. Chem. Phys.
Discussion started: 15 November 2018
© Author(s) 2018. CC BY 4.0 License.

Atmospheric Chemistry and Physics Discussions

3.2 Isotope Modelling

The isotopic composition can be expressed in delta values, in units of per mil (‰). The small delta (δ) is the isotopic ratio R (heavy C / light C) of a sample relative to the isotope ratio of a standard substance (Equation 2, Stuiver & Polach (1977)).

$$\delta^{14}C = \left[\frac{{}^{14}C\ sample / C\ sample}{{}^{14}C\ std / C\ std} - 1 \right] \times 1000 \quad (2)$$

Here, ^{14}C sample is the ^{14}C content of sample, C sample is the carbon content of sample, ^{14}C std is the ^{14}C content of standard and C standard is the carbon content of standard.

Unstable ^{14}C can also be expressed as capital delta Δ^{14}C (Equation 3, (Stuiver and Polach, 1977)). The Δ^{14}C is normalized to a δ^{13}C value of -25 ‰, this is done to account for fractionation. Fractionation effects discriminate against ^{14}C twice as much as for ^{13}C (Stuiver and Polach, 1977). Normalising ^{14}C measurements to a common δ^{13}C should, therefore, remove reservoir specific differences caused by fractionation,

$$\Delta^{14}C = \delta^{14}C - 2 \times (\delta^{13}C + 25) \times \left(1 + \frac{\delta^{14}C}{1000}\right) \quad (3)$$

where δ^{14}C is ^{14}C signature [‰] and δ^{13}C is ^{13}C signature [‰].

For this work, sector-specific emissions reported in EDGAR v4.2 from year 2010 (Olivier et al., 2014) were used for the simulations of anthropogenic emissions and the National Aeronautics and Space Administration Carnegie Ames Stanford Approach (NASA CASA) emissions for biogenic emissions (Potter, 1999). It is assumed that all emissions reported in EDGAR correspond to $^{12}CO_2$ emissions. A detailed list of source sectors and associated isotopic signatures can be found in the supplementary data (S2). All fossil sources were considered to have a $\Delta^{14}CO_2$ value of -1000 ‰. The $^{13}CO_2$ was calculated with equation 4, it is a rearranged version of the definition of the δ value given in equation 2. For the simulations of $\delta^{13}CO_2$ values, the $^{13}CO_2$ from individual source sectors, calculated with equation 4, were integrated together in equation 5. Similarly, the $^{14}CO_{2\,i}$ was calculated by combining the definition of the $\Delta^{14}CO_2$ value from equation 3 with the definition of the δ value from equation 2 and solving for $^{14}CO_2$ (Equation 6). Subsequently, the $^{14}CO_{2\,i}$ from each source sector was added together resulting in the modelled $\Delta^{14}CO_2$ value (Equation 7).

$${}^{13}CO_{2\,i} = \left(\frac{\delta^{13}CO_{2\,i}}{1000} + 1 \right) \times \ CO_{2\,i} \times {}^{13}R_{ref} \quad (4)$$

$$\delta^{13}CO_2 = \left(\frac{\frac{\sum {}^{13}CO_{2\,i} + {}^{13}CO_{2\,bg}}{CO_2}}{{}^{13}R_{ref}} - 1 \right) \times 1000 \quad (5)$$

Here, $^{13}CO_{2\,i}$ is the abundance $^{13}CO_2$ from sector i [mol mol^{-1}], $\delta\,^{13}CO_{2\,i}$ is $^{13}CO_2$ signature sector i [‰], $CO_{2\,i}$ = abundance CO_2 from sector i [mol mol^{-1}], $^{13}R_{ref}$ is the ratio of reference standard [(mol mol^{-1})/ (mol mol^{-1})] and CO_2 is the total abundance CO_2 enhancement [mol mol^{-1}] from Equation 1.

Atmos. Chem. Phys. Discuss., https://doi.org/10.5194/acp-2018-1042
Manuscript under review for journal Atmos. Chem. Phys.
Discussion started: 15 November 2018
© Author(s) 2018. CC BY 4.0 License.

$$^{14}CO_{2\,i} = \frac{-(\Delta^{14}CO_{2\,i}+1000)\times CO_{2\,i}\times {}^{14}R_{ref}}{2\times(\delta^{13}CO_{2\,i}-475)} \quad (6)$$

$$\Delta^{14}CO_2 = \left(\frac{\sum \frac{^{14}CO_{2\,i}}{CO_2}\times\left(1-2*\frac{25+\delta^{13}CO_2}{1000}\right)}{^{14}R_{ref}} - 1\right)\times 1000 \quad (7)$$

Where, $^{14}CO_{2\,i}$ is the abundance $^{14}CO_2$ from sector i [mol mol^{-1}], $\Delta\,^{14}CO_{2\,i}$ is the $^{14}CO_2$ signature sector i [‰], $^{12}CO_{2\,i}$ is the abundance CO_2 from sector i [mol mol^{-1}], $^{14}R_{ref}$ is the ratio of reference standard [(mol mol^{-1})/ (mol mol^{-1})], $^{12}CO_2$ is the total abundance CO_2 enhancement [mol mol^{-1}] from Equation 1 and $\delta\,^{13}CO_2$ is the $^{13}CO_2$ signature [‰] from Equation 5.

3.3 Determination of fossil fuel CO_2

The observed atmospheric mole fraction of CO_2 can be described as the sum of emissions from individual sectors and a background contribution (Equation 8). In Equation 9, the isotopic composition of the observed air is calculated by weighting each sector's contribution with its $\Delta^{14}CO_2$ signature. Where CO_{2_i} describes the mole fraction contribution and Δ_i the $\Delta^{14}CO_2$ ratio from each sector. In this very simple form, the sectors included are: Observed (obs), background (bg), biospheric (bio) and fossil fuel burning (ff), other sectors can be added.

$$CO_{2\,obs} = CO_{2\,bg} + CO_{2\,bio} + CO_{2\,ff} \quad (8)$$

$$CO_{2\,obs}\,\Delta_{obs} = CO_{2\,bg}\,\Delta_{bg} + CO_{2\,bio}\Delta_{bio} + CO_{2\,ff}\Delta_{ff} \quad (9)$$

Multiple ways to solve for the fossil fuel mole fraction $ffCO_2$ are used in the literature, this study follows the approach from (Turnbull et al., 2009) shown in Equation 10, where it is assumed that Δ_{bio} is equal to Δ_{obs}. The reason for this assumption is explained in the next paragraph. The Turnbull et al., 2009 equation is chosen as it separates the calculation of the $ffCO_2$ from any corrections (Δ_{other}) that need to be applied. Multiple corrections can be added individually, and their impact assessed.

$$CO_{2\,ff} = \frac{CO_{2\,bg}\,(\Delta_{obs}-\Delta_{bg})}{(\Delta_{ff}-\Delta_{obs})} - \frac{CO_{2\,other}\,(\Delta_{other}-\Delta_{obs})}{(\Delta_{ff}-\Delta_{obs})} \quad (10)$$

3.3.1 Biospheric correction

$^{14}CO_2$ is constantly produced in the atmosphere, carbon pools, that exhibit a reasonably fast exchange rate with the atmosphere, therefore were in equilibrium with the atmosphere. This equilibrium was disturbed by the addition of large amounts of ^{14}C into the atmosphere by nuclear bomb testing (1950s-1960s). This caused a rapid increase in the $^{14}CO_2$ content of the atmosphere, commonly referred to as the bomb spike (Levin et al., 1980; Manning et al., 1990). The amount of $^{14}CO_2$ in the atmosphere has been decreasing since 1963, as it has been assimilated into other carbon pools. Because of this, the ^{14}C content of the biosphere, the ocean and the atmosphere is still in a disequilibrium today.

At the time of the study, the biosphere was enriched in ^{14}C compared to the atmosphere. The age (time since assimilation) of the carbon emitted from the biosphere to the atmosphere determines the isotopic signature of biospheric emissions. In this

© Author(s) 2018. CC BY 4.0 License.

work, biospheric emissions were split into two sources, autotrophic and heterotrophic. Autotrophic respiration of plants generally contains recently assimilated carbon (<1 year). Therefore, $^{14}CO_2$ from autotrophic respiration is generally assumed to be in equilibrium with the atmosphere and is defined as being equal to Δ_{obs} for Equation 10. While recent work has indicated that autotrophic respiration may also contain older carbon (Phillips et al., 2015), it is assumed to be negligible for this work. Heterotrophically respired CO_2 contains carbon from older pools (for example decaying biomass) and can be significantly enriched in ^{14}C compared to current atmospheric CO_2 (Naegler and Levin, 2009). To simulate the $\Delta^{14}CO_2$ from heterotopic respiration (RH), the 1-box model developed by (Graven et al., 2012) was used, it is assumed that two-thirds of heterotrophic respiration originates from older carbon pools. This resulted in a $\Delta^{14}CO_{2RH}$ of 67-91‰ for 2014-2015, and therefore a value of 80‰ was utilised in all calculations.

3.3.2 Nuclear correction

Radiocarbon emissions from nuclear reactors can have a large temporal variability, making them difficult to correct for. Although the emissions are small, they have a $\Delta^{14}C$ value of ~10^{15}‰, and can, therefore, influence radiocarbon observations significantly. During the study period, 3 types of nuclear power plants were in operation in the UK (figure 1). Of these, both the AGR and the Magnox Reactor are cooled with CO_2 gas. This creates an oxidising condition in the reactor, resulting in the majority of the released ^{14}C being released in the form of $^{14}CO_2$. It is produced in the reactor from reactions of neutrons with ^{14}N, ^{13}C, ^{17}O. Most of the $^{14}CO_2$ emitted from the AGRs and Magnox plants originates from N_2 impurities in the cooling gas (Yim and Caron, 2006). The UK also has one running pressurised water reactor (PWR), Sizewell B (52.21 °N, 1.62 °E), in the east of England. They contain a reducing reactor environment, leading to ^{14}C being released predominantly in the form of $^{14}CH_4$. As ^{14}C is constantly produced in nuclear reactors, parameterized emissions are a good approximation. However, the production of ^{14}C is highly dependent on the number of impurities present in the reactor and only a small part of the produced ^{14}C is ever emitted. Emissions can be caused by leakage as well as operational procedures, known as blowdown events. Reported emissions are therefore more informative. For the correction, a ^{14}C emissions map was created with the highest frequency data available from each nuclear site. Monthly atmospheric emission data were provided by the two operators of the ten UK nuclear power plants; EDF and Magnox Ltd. Data for the of other seventeen UK nuclear sites were taken from the annual Radioactivity in Food and the Environment RIFE, 1995-2016 (Enviroment Agency, Natural Resources Wales, 2017). The emissions from other European nuclear power plants were sourced from annual environmental reports if available (France, Germany) otherwise parameterized emissions were calculated according to (Graven and Gruber, 2011). The largest emitter of ^{14}C in Europe is the nuclear fuel reprocessing site in La Hague, Northern France (49.68 °N, 1.88 °W). For La Hague, monthly emission data reported on their website were utilised and is included in the supplementary material (S3).

4 Results

4.1 Biospheric and nuclear correction

© Author(s) 2018. CC BY 4.0 License.

The biospheric and nuclear corrections were calculated and their magnitude compared. Figure 2 contains the modelled biospheric and nuclear corrections applicable over the whole study period 2014-2015 displayed as $ffCO_2$ equivalent, points represent times flask samples were taken. The mean correction was 0.4 ppm $ffCO_2$ equivalent for the heterotrophic respiration and 0.3ppm for the nuclear emissions. This means that the average nuclear correction at TAC for $^{14}CO_2$ derived $ffCO_2$ is similar in magnitude to the correction for heterotrophic respiration. However, the highest values calculated for the nuclear correction were 3.5 ppm $ffCO_2$ equivalent, almost 4 times larger than the highest biospheric value (1ppm). For the nuclear correction, La Hague and Sizewell have the largest influence on the air parcels arriving at TAC, La Hague because it is the highest emitter, and Sizewell as it is spatially close, 50 km south east of TAC.

Generally, the corrections applied for the heterotrophic respiration and the nuclear industry emissions are much smaller than the measurement uncertainty (combined measurement uncertainty ± 5 ‰ ~ 1.8 ppm CO_2 equivalent). The observed $ffCO_2$ signal in TAC is frequently (50% of observations) smaller than the measurement uncertainty of the radiocarbon method. Two values observed in November 2014 show a larger depletion in $^{14}CO_2$, leading to a strong $ffCO_2$ signal. These two observations coincide with a CO_2 enhancement that lasted approximately two weeks, which can be observed in Figure 3. Footprints calculated during this period indicate that the high CO_2 values are associated with an accumulation of emissions from a large geographical area over the UK and North-West Europe, due to an extended period of low wind speeds. The model appears to significantly underestimate the amplitude of this peak. Therefore, this period was excluded from our analysis, as it is so large that it distorts the interpretation of all the other observations, and it is likely that the model would not represent these conditions well.

4.2 Comparison of modelled and observed data

For this work $^{12}CO_2$, $^{13}CO_2$ and $^{14}CO_2$ were simulated at TAC and are compared with observations in Figure 3. Daily mean values are displayed for both the modelled (blue line) and the observed data (black line, points). The uncertainty estimate (light blue area) includes the baseline uncertainty as well as the emission inventory uncertainty. The uncertainties were investigated by calculating a Monte Carlo ensemble of model runs (4000 runs) with perturbed background concentrations and sector-specific emissions. The background concentration was randomly altered within a factor of two of the measurement uncertainty. The sector-specific emission maps were multiplied with a randomly generated matrix, that let the emission in each grid cell vary between 50 – 150%. The shaded blue areas represent the 95 % confidence interval uncertainty of these simulations. The TAC observations generally match the simulations well for $^{12}CO_2$ and $^{14}CO_2$. The exception is a large $^{12}CO_2$ peak in November 2014 that is significantly underestimated by the model. During the same time period, the two $^{14}CO_2$ samples taken were more depleted than the $^{14}CO_2$ simulations.

The $^{13}CO_2$ simulations show comparatively large uncertainties, the investigation showed that much of the uncertainty was due to the net ecosystem exchange flux. For the $^{14}CO_2$ simulations, the calculated uncertainty estimate of ± 5 ‰ (~ 2 ppm $ffCO_2$

© Author(s) 2018. CC BY 4.0 License.

equivalent) was predominantly influenced by the perturbation of the background concentration (> ± 4 ‰). The average above-baseline enhancement is 4 ‰ (~ 2.9 ppm $ffCO_2$ equivalent). This is not surprising as the $\Delta\ ^{14}CO_2$ observations have a large measurement uncertainty (1.8 ‰, ~ 0.72 ppm $ffCO_2$ equivalent) associated with them, and the measurement uncertainty was chosen as an indication of the background uncertainty. However, it emphasizes that strong $ffCO_2$ signals are needed in order to obtain $\Delta\ ^{14}CO_2$ observations that can be distinguished from the background. At TAC, the fossil fuel influence is not always large enough to break this threshold.

4.3 Fossil Fuel CO_2

The amount of $ffCO_2$ at TAC was calculated using equation 10, 1 ppm of $ffCO_2$ causes a depletion of approximately 2.5 ‰ in $\Delta^{14}CO_2$. On the 13 June 2014, a value of over 50 ‰ was observed, which is significantly larger than the background value of around 21 ‰ at the time. This enhancement in $\Delta^{14}CO_2$ is likely to be caused by nuclear emissions (no forest fires were reported in the area). However, the reported monthly emissions from nuclear sites cannot adequately correct for this, even though air masses were originating from the North West of England where two nuclear power plants (Heysham 1&2 (54.03 °N, 2.92 °W)) and a nuclear fuel processing site (Sellafield (54.42 °N, 3.50 °W)) are situated. Maintenance work requiring reactor shut down can be emission intensive, but this variability is not picked up by the reported monthly emissions. Heysham 1 was shut down for an in-depth boiler inspection (Office for Nuclear Regulation, 2014) on the 10 July 2014 and could be a possible cause of this discrepancy. The measurement on 13 June 2014 was excluded from further analysis. Most observed values are not significantly different from the modelled values. This implies there the $ffCO_2$ derived from the ^{14}C method agrees well with the values simulated using emissions inventories and an atmospheric model. However, as the uncertainties associated with both the simulation as well as the ^{14}C method are large while the $ffCO_2$ emissions from the UK are relatively low. This means that in the UK only very large deviations from the emission inventories would be captured by the ^{14}C-derived $ffCO_2$ method. Carbon monoxide (CO) is a product of incomplete combustion and as such is co-emitted with the CO_2 produced by complete combustion. CO emissions can be expressed as a ratio relative to the fossil fuel CO_2 emissions. The emitted CO / CO_2 ratio varies depending on the emission source. According to the NAEI 2014, UK gas power plants (1.0 ppb(CO) $ppm(CO_2)^{-1}$) and diesel cars (0.5 ppb(CO) $ppm(CO_2)^{-1}$) have low emission ratios, while petrol operated trucks can have an emission ratio as high as 80.0 ppb ppm^{-1}. $\Delta^{14}CO_2$-derived $ffCO_2$ is an expensive measurement often performed at low temporal resolution. Therefore, to maximise the scientific value of low frequency $ffCO_2$ observations, $ffCO_2$ has been used to calibrate the CO_{enh} / $ffCO_2$ ratio for an individual sampling site (CO_{enh} = CO_{obs}-CO_{bg}) (Levin and Karstens, 2007; Miller et al., 2012; Turnbull et al., 2006). The 15th percentile of the MHD CO data was used as the background (CO_{bg}). For CO_{obs}, time-matched TAC observations from the 100 m inlet line were used. For the simulations, CO emissions estimates came from the NAEI 2012 and $ffCO_2$ from EDGAR 2010. EDGAR was used for $ffCO_2$ for consistency of source sectors over the whole modelling domain.

© Author(s) 2018. CC BY 4.0 License.

To estimate the uncertainty associated with the linear regression, the data were randomly resampled 10000 times, the values were allowed to vary within the measurement uncertainty. Figure 5 shows the CO_{enh} in TAC versus the observed $ffCO_2$ from the $^{14}CO_2$ method, a list of the results can be found in table 2. The median of the ratio was 5.7 (2.4-8.9) ppb ppm^{-1}, with a median R^2 correlation coefficient of 0.50. The $ffCO_2$ uncertainty was estimated at 1.8 ppm and for CO_{enh}, 2 ppb. Including the large fossil fuel peak in November 2014 leads to a much stronger correlation (R^2 = 0.85) but a similar ratio of 6.5 (4.8-7.9) ppb ppm^{-1}. The CO/$ffCO_2$ ratio is often described as more robust in winter because the fossil fuel fluxes are larger, minimising the influence of CO from biogenic sources. Including all data points in winter leads to a value of 6.6 (4.6-8.0) ppb ppm^{-1}, and excluding the November peak to 4.7 (1.0-10.1) ppb ppm^{-1}. The ratio using all data values is similar to the simulated ratio of 5.1 ppb ppm^{-1} for TAC. However, it is important to note that, in reality, the individual CO : $ffCO_2$ ratio varies for every measurement. This is because at each point in time, the station can be influenced by different combinations of each sector, each with emission ratio that may vary significantly with time. The sector-specific simulations, included in the supplementary material (S3), show that one of the dominant emission source sectors observable at TAC is road transport, an emission source with an inherently large variability in CO : $ffCO_2$ emissions. The CO : $ffCO_2$ emission ratio is dependent on fuel type, type of car and how it is driven (more emissions during cold starts and stop - start as opposed to a constant speed).

If we apply the simple average ratio to the CO data, it leads to enhancements that is significantly larger than the model. A possible reason for the variability in the observed CO ratio compared with the inventory is the lack of spatiotemporal resolution of the emission inventory. The $^{14}CO_2$ derived CO : $ffCO_2$ ratio and the high-frequency CO observations at TAC are used to estimate a high-frequency $ffCO_2$ time-series. This results in $ffCO_2$ peaks that are significantly higher than values simulated using the EDGAR 2010 inventory (Supplementary material S5). However, EDGAR does not have a seasonal or diurnal cycle, therefore, may not be able to capture the variability on the small timescales examined here.

5 Discussion

In other global locations without large $ffCO_2$ emissions, integrated samples over weeks or months are used to increase the signal strength. In the UK, however, this would not be easily applicable as both the fossil fuel and nuclear signals would be integrated. The correction would then be difficult to apply, as the duration of the sampling would increase the chances of a routine blowdown or a maintenance event occurring at a nuclear reactor nearby. The outcomes of this study, lead to the recommendation of using 3-hour integrated air samples similar to Turnbull et al., 2012, with an automated sampling trigger for ideal sampling conditions, in a location slightly closer to the sources. Choosing a sampling site that is closer to high emitting regions (Figure 6) would provide more sampling times suitable for the radiocarbon method. A 1 year forward run was performed in NAME for both CO and $^{14}CO_2$ (June 2012-June 2013) to find suitable sampling locations in the UK. CO was used as a proxy for fossil fuel CO_2. The conversion factor of 5.7 ppb $ppm^{-1,}$ determined in this work, was used to convert CO into CO_2. The lower the ratio, the more suited is the location for radiocarbon measurements. Although providing national estimations of fossil fuel emissions is vital, the application of $^{14}CO_2$ may be better suited to city scale estimations. This would

© Author(s) 2018. CC BY 4.0 License.

optimise the scientific value of ^{14}C derived $ffCO_2$ estimation. With the provision of higher frequency nuclear power station emission data in the UK and improvements to the biospheric correction, uncertainties associated with $ffCO_2$ calculations could be reduced, improving the usability of this method in the UK.

6 Conclusions

This study of $^{14}CO_2$ measurements has provided a valuable insight into the viability of these type of measurements in the UK. It has shown, the UK fossil fuel emissions estimates from EDGAR are consistent with the observations. The derived $ffCO_2$: CO ratio is consistent with the inventory. Although, uncertainties are large and it appears much of the variability may not be accounted for, by using a simple ratio. Despite the comparatively high density of $^{14}CO_2$ emitting nuclear reactors, corrections applied for nuclear emissions are not generally larger than those applied to account for the biospheric disequilibrium. However, both corrections add to the uncertainty of observed $ffCO_2$ values. The largest issue with using $^{14}CO_2$ observations at TAC for national emission estimates is that the measurement uncertainty is often higher than the observed and predicted depletion in radiocarbon. The use of radiocarbon to estimate UK emissions could be improved in various ways. Higher frequency and automated samples would be one way to address this. Samples could be stored to allow for assessment of their back trajectories and mole fraction information of trace compounds before $^{14}CO_2$ analysis.

7 Author Contribution

Angelina Wenger developed the sampling equipment, oversaw the measurements and carried out the research. Simon O'Doherty and Angelina Wenger designed the research. Katherine Pugsley and Angelina Wenger ran the simulations. Simon O'Doherty provided CO_2 and CO data. Alistair Manning, Matt Rigby, Mark Lunt and Emily White ran NAME simulations and analysed of the model output. Katherine Pugsley and Angelina Wenger prepared the manuscript with contributions from all co-authors.

8 Acknowledgements

The authors would like to acknowledge Scott Lehman, Chad Wolak, Stephen Morgan and Patrick Cappa of the INSTAAR Laboratory for Radiocarbon Preparation and Research for the ^{14}C sample processing and Don Neff and the NOAA GMD team for the routing of the samples as well as the greenhouse gas analysis. Collection of radiocarbon measurements was funded by the NERC GAUGE programme under a grant to the University of Bristol NE/K002236/1.

References

Andres, R., Marland, G., Boden, T. and Bischof, S.: Carbon dioxide emissions from fossil fuel consumption and cement manufacture, 1751–1991, and an estimate of their isotopic composition and latitudinal distribution, 1993 Global Change Institute Cambridge Univ. Press, New York., 1994.

© Author(s) 2018. CC BY 4.0 License.

Ballantyne, A. P., Andres, R., Houghton, R., Stocker, B. D., Wanninkhof, R., Anderegg, W., Cooper, L. A., DeGrandpre, M., Tans, P. P., Miller, J. B., Alden, C. and White, J. W. C.: Audit of the global carbon budget: Estimate errors and their impact on uptake uncertainty, Biogeosciences, 12(8), 2565–2584, doi:10.5194/bg-12-2565-2015, 2015.

Balzani Lööv, J. M., Henne, S., Legreid, G., Staehelin, J., Reimann, S., Prévôt, A. S. H., Steinbacher, M. and Vollmer, M. K.: Estimation of background concentrations of trace gases at the Swiss Alpine site Jungfraujoch (3580 m asl), J. Geophys. Res. Atmos., 113(22), 1–17, doi:10.1029/2007JD009751, 2008.

Barlow, J. M., Palmer, P. I., Bruhwiler, L. M. and Tans, P.: Analysis of CO2 mole fraction data: First evidence of large-scale changes in CO2 uptake at high northern latitudes, Atmos. Chem. Phys., 15(23), 13739–13758, doi:10.5194/acp-15-13739-2015, 2015.

BEIS, U.: Final UK Greenhouse gas emissions national statistic:1990-2016 (2016 UK ghg:final figures-statistical release), Dep. Business, Energy Ind. Strateg., (February) [online] Available from: https://www.gov.uk/government/statistics/final-uk-greenhouse-gas-emissions-national-statistics-1990-2016, 2018.

Berhanu, T. A., Szidat, S., Brunner, D., Satar, E., Schanda, R., Nyfeler, P., Battaglia, M., Steinbacher, M., Hammer, S. and Leuenberger, M.: Estimation of the fossil fuel component in atmospheric CO2 based on radiocarbon measurements at the Beromünster tall tower, Switzerland, Atmos. Chem. Phys., 17(17), 10753–10766, doi:10.5194/acp-17-10753-2017, 2017.

Bozhinova, D., Van Der Molen, M. K., Van Der Velde, I. R., Krol, M. C., Van Der Laan, S., Meijer, H. A. J. and Peters, W.: Simulating the integrated summertime δ14CO2 signature from anthropogenic emissions over Western Europe, Atmos. Chem. Phys., 14(14), 7273–7290, doi:10.5194/acp-14-7273-2014, 2014.

Bozhinova, D., Palstra, S. W. L., van der Molen, M. K., Krol, M. C., Meijer, H. A. J. and Peters, W.: Three Years of Δ14CO2 Observations from Maize Leaves in the Netherlands and Western Europe, Radiocarbon, 58(03), 459–478, doi:10.1017/RDC.2016.20, 2016.

Ciais, P., Tans, P. P., Trolier, M., White, J. W. C. and Francey, R. J.: A Large Northern Hemisphere Terrestrial CO2 Sink Indicated by the 13C/12C Ratio of Atmospheric CO2, Science (80-.)., 269(5227), 1098–1102, doi:10.1126/science.269.5227.1098, 1995.

Ciais, P., Paris, J. D., Marland, G., Peylin, P., Piao, S. L., Levin, I., Pregger, T., Scholz, Y., Friedrich, R., Rivier, L., Houwelling, S. and Schulze, E. D.: The European carbon balance. Part 1: Fossil fuel emissions, Glob. Chang. Biol., 16(5), 1395–1408, doi:10.1111/j.1365-2486.2009.02098.x, 2010.

Currie, L. A.: The remarkable metrological history of radiocarbon dating [II], J. Res. Natl. Inst. Stand. Technol., 109(2), 185, doi:10.6028/jres.109.013, 2004.

Enviroment Agency, Natural Resources Wales, F. S. A.: RIFE reports, [online] Available from: https://www.gov.uk/government/publications/radioactivity-in-food-and-the-environment-rife-reports-2004-to-2016, 2017.

Friedlingstein, P., Houghton, R. A., Marland, G., Hackler, J., Boden, T. A., Conway, T. J., Canadell, J. G., Raupach, M. R., Ciais, P. and Le Quéré, C.: Update on CO2 emissions, Nat. Geosci., 3(12), 811–812, doi:10.1038/ngeo1022, 2010.

Gamnitzer, U., Karstens, U., Kromer, B., Neubert, R. E. M., Meijer, H. A. J., Schroeder, H. and Levin, I.: Carbon monoxide:

© Author(s) 2018. CC BY 4.0 License.

A quantitative tracer for fossil fuel CO<inf>2</inf>?, J. Geophys. Res. Atmos., 111(22), 1–19, doi:10.1029/2005JD006966, 2006.

Graven, H. D. and Gruber, N.: Continental-scale enrichment of atmospheric14CO2from the nuclear power industry: Potential impact on the estimation of fossil fuel-derived CO2, Atmos. Chem. Phys., 11(23), 12339–12349, doi:10.5194/acp-11-12339-2011, 2011.

Graven, H. D., Guilderson, T. P. and Keeling, R. F.: Observations of radiocarbon in CO<inf>2</inf> at la Jolla, California, USA 1992-2007: Analysis of the long-term trend, J. Geophys. Res. Atmos., 117(2), 1–14, doi:10.1029/2011JD016533, 2012.

Gurney, K. R., Liang, J., Patarasuk, R., O'Keeffe, D., Huang, J., Hutchins, M., Lauvaux, T., Turnbull, J. C. and Shepson, P. B.: Reconciling the differences between a bottom-up and inverse-estimated FFCO2 emissions estimate in a large US urban area, Elem Sci Anth, 5(0), 44, doi:10.1525/elementa.137, 2017.

IPCC: Summary for Policymakers., 2014.

Jones, A., Thomson, D., Hort, M. and Devenish, B.: The U . K . Met Office ' s next generation atmospheric dispersion model, NAME III, UK Met Off., 1–8, 2007.

Lehman, S. J., Miller, J. B., Wolak, C., Southon, J. R., Trans, P. P., Montzka, S. a., Sweeney, C., Andrews, A., LaFranchi, B., Guilderson, T. P. and Turnbull, J. C.: Allocation of terrestrial carbon sources using \ce{^{14}CO2}: Methods, measurement, and modeling, Radiocarbon, 55(2–3), 1484–1495, doi:10.2458/azu_js_rc.55.16392, 2013.

Levin, I. and Karstens, U.: Inferring high-resolution fossil fuel CO2 records at continental sites from combined 14CO2 and CO observations, Tellus, Ser. B Chem. Phys. Meteorol., 59(2), 245–250, doi:10.1111/j.1600-0889.2006.00244.x, 2007.

Levin, I. and Kromer, B.: Twenty Years of Atmospheric 14CO2 Observations at Schauinsland Station, Germany, Radiocarbon, 39(2), 205–218, doi:10.2458/azu_js_rc.39.1942, 1997.

Levin, I., Munnich, K. and Weiss, W.: the Effect of Anthropogenic Co2 and C-14 Sources on the Distribution of C-14 in the Atmosphere, Radiocarbon, 22(2), 379–391, doi:10.2458/azu_js_rc.22.627, 1980.

Levin, I., Kromer, B., Schmidt, M. and Sartorius, H.: A novel approach for independent budgeting of fossil fuel CO_2 over Europe by $^{14}CO_2$ observations, Geophys. Res. Lett., 30(23), n/a-n/a, doi:10.1029/2003GL018477, 2003.

Lopez, M., Schmidt, M., Delmotte, M., Colomb, A., Gros, V., Janssen, C., Lehman, S. J., Mondelain, D., Perrussel, O., Ramonet, M., Xueref-Remy, I. and Bousquet, P.: CO, NOxand13CO2as tracers for fossil fuel CO2: Results from a pilot study in Paris during winter 2010, Atmos. Chem. Phys., 13(15), 7343–7358, doi:10.5194/acp-13-7343-2013, 2013.

Lunt, M. F., Rigby, M., Ganesan, A. L. and Manning, A. J.: Estimation of trace gas fluxes with objectively determined basis functions using reversible-jump Markov chain Monte Carlo, Geosci. Model Dev., 9(9), 3213–3229, doi:10.5194/gmd-9-3213-2016, 2016.

Manning, M. R., Lowe, D. C., Melhuish, W. H., Sparks, R. J., Wallace, G., Brenninkmeijer, C. A. M. and McGill, R. G.: THE USE OF RADIOCARBON MEASUREMENTS IN ATMOSPHERIC STUDIES, Radiocarbon, 32(1), 37–58, 1990.

Miller, J. B., Lehman, S. J., Montzka, S. A., Sweeney, C., Miller, B. R., Karion, A., Wolak, C., Dlugokencky, E. J., Southon, J., Turnbull, J. C. and Tans, P. P.: Linking emissions of fossil fuel CO_2 and other anthropogenic trace gases using atmospheric

© Author(s) 2018. CC BY 4.0 License.

[14] CO 2, J. Geophys. Res. Atmos., 117(D8), n/a-n/a, doi:10.1029/2011JD017048, 2012.

Naegler, T. and Levin, I.: Observation-based global biospheric excess radiocarbon inventory 1963-2005, J. Geophys. Res. Atmos., 114(17), 1–8, doi:10.1029/2008JD011100, 2009.

Nisbet, E. and Weiss, R.: Top-Down Versus Bottom-Up, , 328(June), 1241–1244, 2010.

Office for Nuclear Regulation: Office for Nuclear Regulation (ONR) Quarterly Site Report for Heysham Power Stations, 2014.

Olivier, J. G. ., Janssens-Maenhout, G., Muntean, M. and Peters, J. A. H. .: Trends in global CO2 emissions: 2014 Report., 2014.

Palmer, P. I., O'Doherty, S., Allen, G., Bower, K., Bösch, H., Chipperfield, M. P., Connors, S., Dhomse, S., Feng, L., Finch, D. P., Gallagher, M. W., Gloor, E., Gonzi, S., Harris, N. R. P., Helfter, C., Humpage, N., Kerridge, B., Knappett, D., Jones, R. L., Le Breton, M., Lunt, M. F., Manning, A. J., Matthiesen, S., Muller, J. B. A., Mullinger, N., Nemiitz, E., O'Shea, S., Parker, R. J., Percival, C. J., Pitt, J., Riddick, S. N., Rigby, M., Sembhi, H., Siddans, R., Skelton, R. L., Smith, P., Sonderfeld, H., Stanley, K., Stavert, A. R., Wenger, A., White, E., Wilson, C. and Young, D.: A measurement-based verification framework for UK greenhouse gas emissions: an overview of the Greenhouse gAs Uk and Global Emissions (GAUGE) project, Atmos. Chem. Phys. Discuss., (February), 1–52, doi:10.5194/acp-2018-135, 2018.

Phillips, C. L., Mcfarlane, K. J., Lafranchi, B., Desai, A. R., Miller, J. B. and Lehman, S. J.: Observations of 14CO2 in ecosystem respiration from a temperate deciduous forest in Northern Wisconsin, , (2), 1–17, doi:10.1002/2014JG002808.Received, 2015.

Potter, C. S.: Terrestrial biomass and the effects of deforestration on the global carbon cycle, Bioscience, 49(10), 769–778, 1999.

Le Quéré, C., Andrew, R. M., Canadell, J. G., Sitch, S., Ivar Korsbakken, J., Peters, G. P., Manning, A. C., Boden, T. A., Tans, P. P., Houghton, R. A., Keeling, R. F., Alin, S., Andrews, O. D., Anthoni, P., Barbero, L., Bopp, L., Chevallier, F., Chini, L. P., Ciais, P., Currie, K., Delire, C., Doney, S. C., Friedlingstein, P., Gkritzalis, T., Harris, I., Hauck, J., Haverd, V., Hoppema, M., Klein Goldewijk, K., Jain, A. K., Kato, E., Körtzinger, A., Landschützer, P., Lefèvre, N., Lenton, A., Lienert, S., Lombardozzi, D., Melton, J. R., Metzl, N., Millero, F., Monteiro, P. M. S., Munro, D. R., Nabel, J. E. M. S., Nakaoka, S. I., O'Brien, K., Olsen, A., Omar, A. M., Ono, T., Pierrot, D., Poulter, B., Rödenbeck, C., Salisbury, J., Schuster, U., Schwinger, J., Séférian, R., Skjelvan, I., Stocker, B. D., Sutton, A. J., Takahashi, T., Tian, H., Tilbrook, B., Van Der Laan-Luijkx, I. T., Van Der Werf, G. R., Viovy, N., Walker, A. P., Wiltshire, A. J. and Zaehle, S.: Global Carbon Budget 2016, Earth Syst. Sci. Data, 8(2), 605–649, doi:10.5194/essd-8-605-2016, 2016.

Le Quéré, C., Andrew, R. M., Friedlingstein, P., Sitch, S., Pongratz, J., Manning, A. C., Ivar Korsbakken, J., Peters, G. P., Canadell, J. G., Jackson, R. B., Boden, T. A., Tans, P. P., Andrews, O. D., Arora, V. K., Bakker, D. C. E., Barbero, L., Becker, M., Betts, R. A., Bopp, L., Chevallier, F., Chini, L. P., Ciais, P., Cosca, C. E., Cross, J., Currie, K., Gasser, T., Harris, I., Hauck, J., Haverd, V., Houghton, R. A., Hunt, C. W., Hurtt, G., Ilyina, T., Jain, A. K., Kato, E., Kautz, M., Keeling, R. F., Klein Goldewijk, K., Körtzinger, A., Landschützer, P., Lefèvre, N., Lenton, A., Lienert, S., Lima, I., Lombardozzi, D., Metzl, N., Millero, F., Monteiro, P. M. S., Munro, D. R., Nabel, J. E. M. S., Nakaoka, S. I., Nojiri, Y., Antonio Padin, X., Peregon,

© Author(s) 2018. CC BY 4.0 License.

A., Pfeil, B., Pierrot, D., Poulter, B., Rehder, G., Reimer, J., Rödenbeck, C., Schwinger, J., Séférian, R., Skjelvan, I., Stocker, B. D., Tian, H., Tilbrook, B., Tubiello, F. N., Laan-Luijkx, I. T. V., Werf, G. R. V., Van Heuven, S., Viovy, N., Vuichard, N., Walker, A. P., Watson, A. J., Wiltshire, A. J., Zaehle, S. and Zhu, D.: Global Carbon Budget 2017, Earth Syst. Sci. Data, 10(1), 405–448, doi:10.5194/essd-10-405-2018, 2018.

Roberts, M. and Southon, J.: A preliminary determination of the absolute 14C/12C ratio of OX-I, Radiocarbon, 49(2), 441–445 [online] Available from: http://darchive.mblwhoilibrary.org/handle/1912/4393, 2007.

Ruckstuhl, A. F., Henne, S., Reimann, S., Steinbacher, M., Vollmer, M. K., O'Doherty, S., Buchmann, B. and Hueglin, C.: Robust extraction of baseline signal of atmospheric trace species using local regression, Atmos. Meas. Tech., 5(11), 2613–2624, doi:10.5194/amt-5-2613-2012, 2012.

Sharp, Z.: Principles of stable isotope geochemistry, edited by Pearson, Pearson., 2007.

Stanley, K. M., Grant, A., O'Doherty, S., Young, Di., Manning, A. J., Stavert, A. R., Gerard Spain, T., Salameh, P. K., Harth, C. M., Simmonds, P. G., Sturges, W. T., Oram, D. E. and Derwent, R. G.: Greenhouse gas measurements from a UK network of tall towers: Technical description and first results, Atmos. Meas. Tech., 11(3), 1437–1458, doi:10.5194/amt-11-1437-2018, 2018.

Stuiver, M. and Polach, H.: Reporting of 14C Data, Radiocarbon, 19(3), 355–363, 1977.

Suess, H.: Radiocarbon Concentration in Modern Wood, Science (80-.)., 122(3166), 415–417, doi:10.1126/science.122.3166.415-a, 1955.

Takahashi, T., Sutherland, S. C., Sweeney, C., Poisson, A., Metzl, N., Tilbrook, B., Bates, N., Wanninkhof, R., Feely, R. A., Sabine, C., Olafsson, J. and Nojiri, Y.: Global sea-air CO_2 flux based on climatological surface ocean pCO_2, and seasonal biological and temperature effects, Deep. Res. Part II Top. Stud. Oceanogr., 49, 1601–1622, doi:10.1016/S0967-0645(02)00003-6, 2002.

Turnbull, J., Rayner, P., Miller, J., Naegler, T., Ciais, P. and Cozic, A.: On the use of $^{14}CO_2$ as a tracer for fossil fuel CO_2: Quantifying uncertainties using an atmospheric transport model, J. Geophys. Res., 114(D22), D22302, doi:10.1029/2009JD012308, 2009.

Turnbull, J., Guenther, D., Karion, A., Sweeney, C., Anderson, E., Andrews, A., Kofler, J., Miles, N., Newberger, T., Richardson, S. and Tans, P.: An integrated flask sample collection system for greenhouse gas measurements, Atmos. Meas. Tech., 5(9), 2321–2327, doi:10.5194/amt-5-2321-2012, 2012.

Turnbull, J. C., Miller, J. B., Lehman, S. J., Tans, P. P., Sparks, R. J. and Southon, J.: Comparison of 14CO2, CO, and SF6 as tracers for recently added fossil fuel CO2 in the atmosphere and implications for biological CO2 exchange, Geophys. Res. Lett., 33(1), 2–6, doi:10.1029/2005GL024213, 2006.

Turnbull, J. C., Karion, A., Fischer, M. L., Faloona, I., Guilderson, T., Lehman, S. J., Miller, B. R., Miller, J. B., Montzka, S., Sherwood, T., Saripalli, S., Sweeney, C. and Tans, P. P.: Assessment of fossil fuel carbon dioxide and other anthropogenic trace gas emissions from airborne measurements over Sacramento, California in spring 2009, Atmos. Chem. Phys., 11(2), 705–721, doi:10.5194/acp-11-705-2011, 2011.

© Author(s) 2018. CC BY 4.0 License.

Turnbull, J. C., Sweeney, C., Karion, A., Newberger, T., Lehman, S. J., Cambaliza, M. O., Shepson, P. B., Gurney, K., Patarasuk, R. and Razlivanov, I.: Journal of Geophysical Research : Atmospheres, , 292–312, doi:10.1002/2014JD022555.Received, 2014.

Vogel, F., Levin, I. and Worthy, D. E. J.: Implications for Deriving Regional Fossil Fuel CO2 Estimates from Atmospheric Observations in a Hot Spot of Nuclear Power Plant 14CO2 Emissions, Radiocarbon, 55(3–4), 1556–1572, doi:10.2458/azu_js_rc.55.16347, 2013.

van Vuuren, D. P., Hoogwijk, M., Barker, T., Riahi, K., Boeters, S., Chateau, J., Scrieciu, S., van Vliet, J., Masui, T., Blok, K., Blomen, E. and Kram, T.: Comparison of top-down and bottom-up estimates of sectoral and regional greenhouse gas emission reduction potentials, Energy Policy, 37(12), 5125–5139, doi:10.1016/j.enpol.2009.07.024, 2009.

Xueref-Remy, I., Dieudonné, E., Vuillemin, C., Lopez, M., Lac, C., Schmidt, M., Delmotte, M., Chevallier, F., Ravetta, F., Perrussel, O., Ciais, P., Bréon, F. M., Broquet, G., Ramonet, M., Gerard Spain, T. and Ampe, C.: Diurnal, synoptic and seasonal variability of atmospheric CO2 in the Paris megacity area, Atmos. Chem. Phys., 18(5), 3335–3362, doi:10.5194/acp-18-3335-2018, 2018.

Yim, M. S. and Caron, F.: Life cycle and management of carbon-14 from nuclear power generation, Prog. Nucl. Energy, 48(1), 2–36, doi:10.1016/j.pnucene.2005.04.002, 2006.

Zhao, Y., Nielsen, C. P. and McElroy, M. B.: China's CO2emissions estimated from the bottom up: Recent trends, spatial distributions, and quantification of uncertainties, Atmos. Environ., 59, 214–223, doi:10.1016/j.atmosenv.2012.05.027, 2012.

Atmos. Chem. Phys. Discuss., https://doi.org/10.5194/acp-2018-1042
Manuscript under review for journal Atmos. Chem. Phys.
Discussion started: 15 November 2018
© Author(s) 2018. CC BY 4.0 License.

Atmospheric Chemistry and Physics Discussions

Species, Site **Instrument**	**Scale** **Operator**
CO_2, TAC Picarro CRDS G2301, in-situ	WMO x2007 University of Bristol
CO, TAC GCMD, in-situ	CSIRO-98 University of Bristol
CO_2, MHD Picarro CRDS G2401, in-situ	WMO x2007 LSCE
CO, MHD RGA, in-situ	CSIRO-98 University of Bristol
CO_2, MHD + TAC NDIR, flask	WMO x2007 NOAA
CO, MHD + TAC Aerolaser VUV fluorimetry flask	WMO x2014 NOAA
$^{13}CO_2$, MHD + TAC IRMS, flask	PDB NOAA, INSTAAR
$^{14}CO_2$, MHD + TAC AMS, flask	NBS Oxalic Acid I NOAA, INSTAAR, UC Irvine

Table 1: Overview of greenhouse gas measurements presented in this paper. The acronyms used to describe instruments are Cavity Ring-Down Spectroscopy (CRDS), Gas Chromatography Mass Detector (GCMD), Residual Gas Analyser (RGA), Nondispersive Infrared Detector (NDIR), Vacuum Ultra Violet (VUV), Infrared Mass Spectrometry (IRMS), Accelerator Mass Spectrometry (AMS).

Data	**R^2**	**ppm / ppb**	**P value**
All	0.9 (0.5-0.9)	6.5 (4.8-7.9)	0.01
All (not Nov)	0.5 (0.2-0.7)	5.7 (2.4-8.9)	0.04
Winter only	1.0 (0.7-1.0)	6.6 (4.6-8.0)	0.03

Atmos. Chem. Phys. Discuss., https://doi.org/10.5194/acp-2018-1042
Manuscript under review for journal Atmos. Chem. Phys.
Discussion started: 15 November 2018
© Author(s) 2018. CC BY 4.0 License.

Winter only (not Nov)	0.7 (0.1-1.0)	4.7 (1.0-10.1)	0.15

Table 2. CO ratios using a MHD 15th-percentile as background value under different times using NAEI 2012 emissions inventory and measurements at TAC. Uncertainties shown are the 5th and 95th percentile.

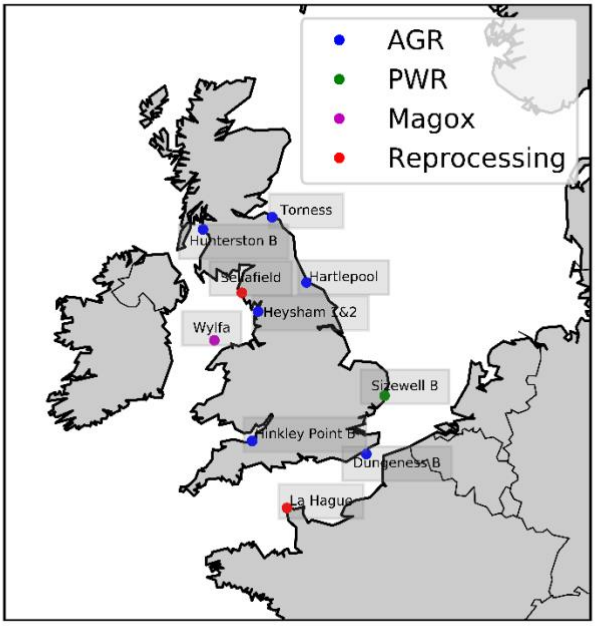

Figure 1. Map of Northern Europe nuclear power stations and other nuclear facilities. Reactor types are: Advanced Gas Reactor (AGR) and Pressurised Water Reactor (PWR), Magnox. Fuel reprocessing are labelled separately.

Atmos. Chem. Phys. Discuss., https://doi.org/10.5194/acp-2018-1042
Manuscript under review for journal Atmos. Chem. Phys.
Discussion started: 15 November 2018
© Author(s) 2018. CC BY 4.0 License.

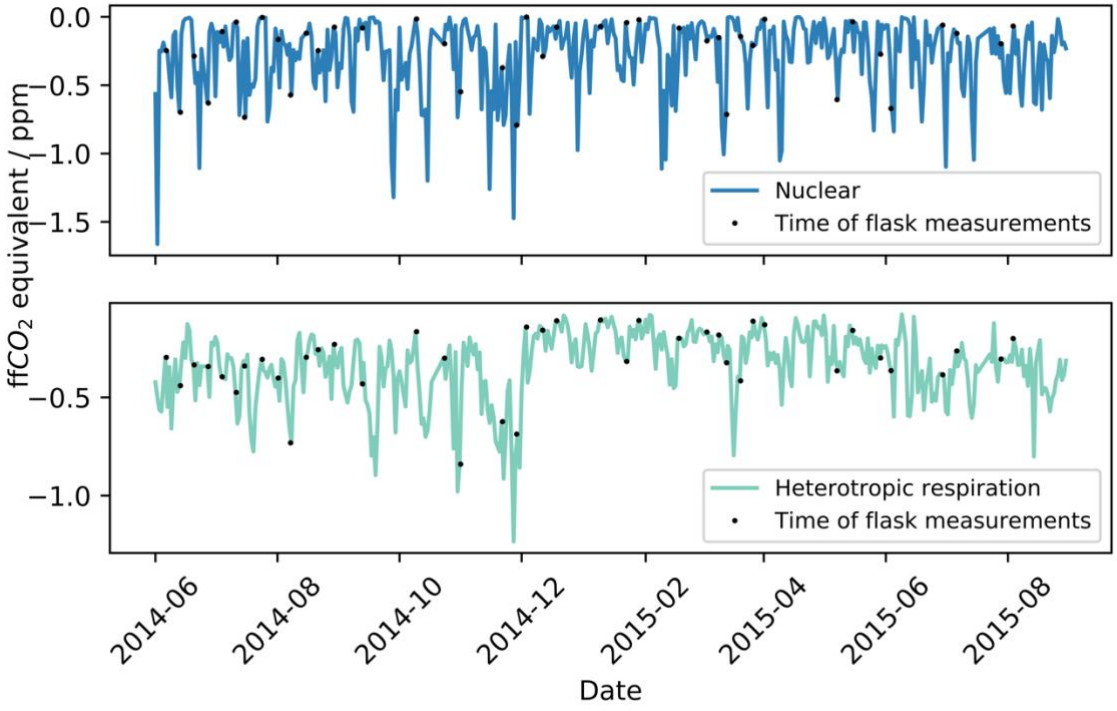

Figure 2: The blue line (top) represents the $ffCO_2$ equivalent theoretical corrections that need to be applied over the whole study period for the nuclear $^{14}CO_2$ emissions. The green line (bottom) represent the $ffCO_2$ equivalent theoretical corrections that need to be applied over the whole study period for heterotrophic respiration from the biosphere. The points represent times flask samples were taken and therefore the corrections that were applied to each measurement.

Atmos. Chem. Phys. Discuss., https://doi.org/10.5194/acp-2018-1042
Manuscript under review for journal Atmos. Chem. Phys.
Discussion started: 15 November 2018
© Author(s) 2018. CC BY 4.0 License.

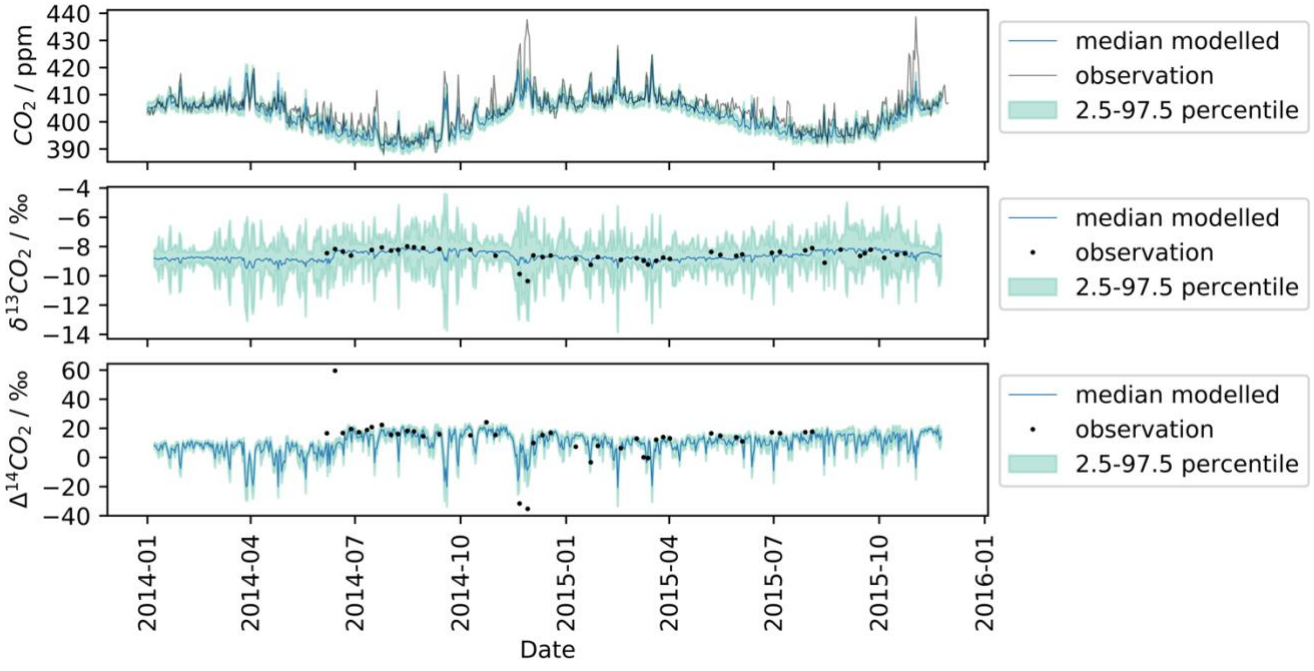

Figure 3: Comparison of modelled and observed CO_2 for each isotope at TAC. a) Simulations of CO_2 in TAC in blue compared with online observations represented in black. b) $^{13}CO_2$ simulations in blue and observations in black points. c) $^{14}CO_2$ modelled in blue compared to observations represented as black points. For all plots, the shaded green area is the 5-95 percentile of the bootstrapping method estimating the uncertainty for the stimulations.

Atmos. Chem. Phys. Discuss., https://doi.org/10.5194/acp-2018-1042
Manuscript under review for journal Atmos. Chem. Phys.
Discussion started: 15 November 2018
© Author(s) 2018. CC BY 4.0 License.

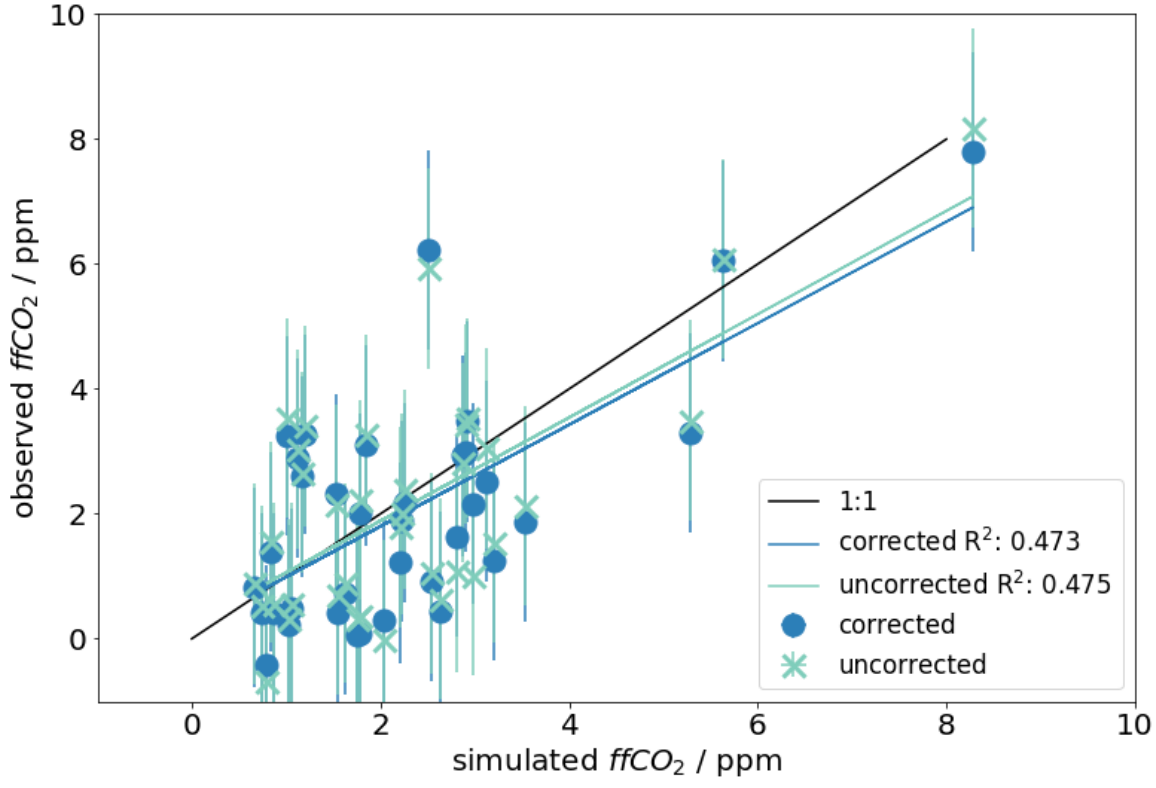

Figure 4: Fossil fuel CO_2 ($ffCO_2$) derived from $^{14}CO_2$ measurements made at TAC, compared to simulated $ffCO_2$ from the NAME model. Due to the potential for high depletion of $^{14}CO_2$ from fossil fuel sources (see Section 4.2), measurements in November 2014 are not shown. Observations that have been corrected for nuclear and biospheric influence are shown as blue points, whereas uncorrected values are shown as turquoise crosses. The 1:1 line is shown in black and linear regression lines for the comparison of the model to the corrected and uncorrected data are shown as blue and turquoise lines, respectively. Error bars = 1.6 ppm.

Atmos. Chem. Phys. Discuss., https://doi.org/10.5194/acp-2018-1042
Manuscript under review for journal Atmos. Chem. Phys.
Discussion started: 15 November 2018
© Author(s) 2018. CC BY 4.0 License.

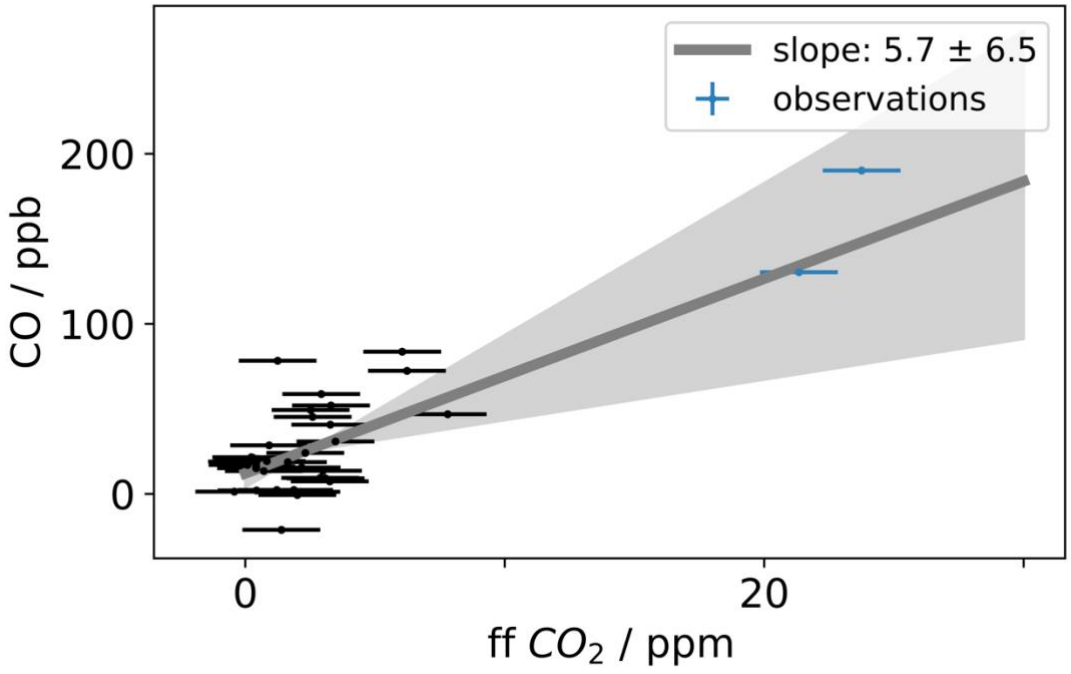

Figure 5. CO_{enh} at TAC against the observed $ffCO_2$ from the $^{14}CO_2$ method points shown in black. In blue are points from November 2014 shown separately because of the high depletion of $^{14}CO_2$ from fossil fuel sources (see Section 4.2). Grey line shows linear regression and grey shading shows the 5-95 % uncertainty. Error bar $ffCO_2$ = 1.6 ppm, error bar CO = 2.0 ppb.

Atmos. Chem. Phys. Discuss., https://doi.org/10.5194/acp-2018-1042
Manuscript under review for journal Atmos. Chem. Phys.
Discussion started: 15 November 2018
© Author(s) 2018. CC BY 4.0 License.

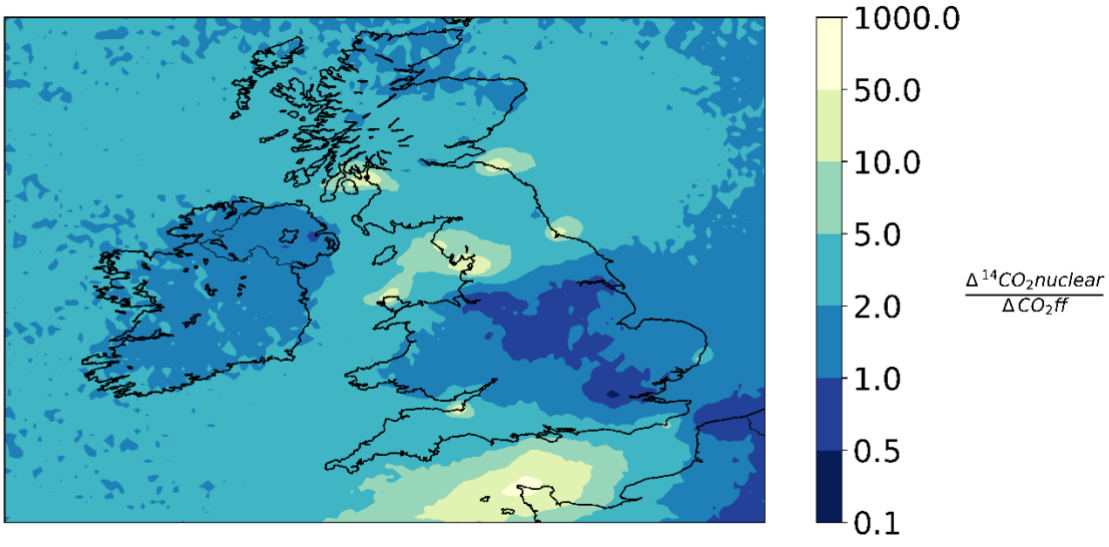

Figure 6. The ratio of $^{14}CO_2$ nuclear to fossil fuel CO_2 to calculated from a 1 year (June 2012 - June 2013) forward run performed in NAME. CO was used as a proxy for $ffCO_2$ and the conversion factor 5.7 ppb ppm^{-1} was used to convert CO to CO_2. High values in yellow represent high nuclear $^{14}CO_2$ influence and low values in blue represent high $ffCO_2$ regions.